

**Title: Effects of 3-D Wave Propagation in Evansville and Impacts on  
Infrastructure**  
USGS Grant G12AP20150

PI: Jennifer S. Haase  
Contributing Author: Lance Ripley  
IGPP, Scripps Institution of Oceanography  
University of California, San Diego  
La Jolla, CA, 92093-0225  
Phone: 858-534-8771, FAX: 858-534-9833, [jhaase@ucsd.edu](mailto:jhaase@ucsd.edu)

Authorized Institutional Representative  
William Park III,  
Scripps Institution of Oceanography  
SIO Contracts Office 0210  
9500 Gilman Drive  
La Jolla, CA 92093-0120  
Phone: 858- 822-1350, [wparkiii@ucsd.edu](mailto:wparkiii@ucsd.edu)

Date: March 31, 2014  
Term of Report: Jan 1, 2013 – Dec 31, 2013

*Abstract*

The Evansville, IN – Henderson, KY urban area is located on the banks of the Ohio River and is within 200-250 km of the New Madrid Fault Zone, which has had repeated large earthquakes over the last 1400 years. The City of Evansville was developed on a sedimentary basin in the Ohio River flood plain. Because of the presence of low shear-wave velocity soils, amplification of seismic waves is expected. The probabilistic estimate of shaking and the probability of occurrence of liquefaction due to a repeat of a New Madrid type event varies significantly over the urban area, based on 1D calculations that considered the 3D variation of depth to bedrock and soil properties. Variations in the acceleration with 2% probability of being exceeded of up to 0.2g at 1s period were calculated across the study area. The objective of this work is to evaluate whether taking into account the three-dimensional nature of the subsurface geology produces significantly different and improved estimations of ground shaking when a 3D wave propagation method is used to estimate ground motions. We have run a series of tests using the Lonestar Supercomputer (TACC, University of Texas) to compare propagation effects in a homogeneous halfspace, a 1D laterally homogeneous model and a 3D model of shallow structure. Because of the large contrast in bedrock and soil velocity, the Courant-Friedrichs-Lewy stability condition required discretization of the model at 25 m for 0.5 Hz simulations and 8 m for 2 Hz simulations. The available bedrock

depth points were re-evaluated in a Geographic Information System to provide a smooth bedrock depth model at this resolution. The aspect ratio of the bedrock valley that separates Indiana from Ohio, is very shallow, and the soil model assumes that deeper than 60 m, the bedrock geology is homogenous, with P-wave velocity 2189 m/s and shear wave velocity of 1251 m/s. The results show that, even with this relatively shallow structure, there is significant amplification as waves are trapped in the river valley. There is a large difference in duration and amplitude of shaking comparing the models with soil layers and without. The general results for both models that have soil layers is that the maximum amplitude of the ground motion is on the order of twice as big as in the homogeneous case, and duration of shaking is also twice as long. We have evaluated the effect of amplification at three sites in the study area where earthquake recordings of a M3.9 earthquake from the New Madrid area are available. The two sites (EVIN and TCIN) that are on deeper soils show amplification at about 2 Hz. Site TCIN, which is located on lacustrine soils, shows an additional amplification peak at around 5-6Hz. These frequencies are consistent with resonance in soils with the range of thicknesses described by the 3D model. EVIN is located above alluvial soils nearby State routes 41 and 62, and is near enough to be representative of soils and site response typical of the conditions for that infrastructure. Three site observations are not sufficient to verify definitively that the 3D response calculated from the soil model, therefore further verification studies should be carried out. However, it indicates the results will be useful for understanding how amplification due to soils may affect major infrastructure in the region.

### *Introduction*

The New Madrid Seismic Zone is located 200 km away from Evansville, Indiana. The New Madrid Seismic Zone is one of the most active seismic regions in the central and eastern United States. In 1811-1812, three large earthquakes (moment magnitudes ranging 7.4 to 8.1) occurred in this region, and were felt throughout the eastern United States. Evansville is settled on the Ohio River terraces and flood plain, above an ancient bedrock valley. Because of low shear-wave velocity soils within the bedrock valley, local amplification of ground motion is expected due to trapped waves. In the Evansville area, 1D calculations have been made (Haase and Nowack, 2011) that demonstrated the importance of the geological near-surface structure in amplifying or not amplifying seismic waves. In that study, wave energy was imposed assuming vertical-only propagation. (Idriss et al., SHAKE91, 1992). A 1D calculation was implemented to map the site amplification in the Evansville area, with the depth to bedrock and soil velocities varying at each point in the study region. In the simulation, the source was located in the New Madrid Seismic Zone, at 180 km away from the city, and was assumed to be similar to the great 1811-1812 New Madrid earthquakes. It was found that local geological characteristics have a very strong effect on the level of ground motion.

To evaluate more precisely the amplification zones that affect the scenario hazard maps, there is a need to carry out 3D calculations so that energy can propagate with sloping interfaces of the bedrock valley and the results can be more

realistic. We will implemented a 3D finite difference calculation, using a fourth-order staggered grid method (Olsen et al., 1995), to propagate a wave in the Evansville region from a source coming vertically to determine the three components of ground motion. Then we evaluated the amplification by comparing it to a simulation in a 1D-varying medium and a homogeneous half space. We start by describing briefly the geological data we use to derive the 3D soil model. Then we explain the governing equations of the wave propagation and the finite difference approach. Steps that were carried out to implement the 3D calculation will be presented, before presenting the results of the simulations: plots of ground motion amplitude at the surface, and record sections of the time series.

### *Data*

To implement an analysis of the soil response, several parameters are required; the most important ones are the bedrock depth, the shear-wave velocity and the density. The surficial geology map (Figure 1, Moore et al., 2009) shows the diversity of the soil types in the Ohio River flood plain: low terrace outwash alluvium and lacustrine deposits mainly. Away from the Ohio River, soils are loess and lacustrine terrace slackwater deposits. A bedrock depth model has been produced based on water well logs (Bleuer, 2000), depth measurements interpreted from P-wave refraction profiles (Rudman and others, 1973; Whaley and others, 2002), and bedrock elevation points from oil, gas, and water well logs. The model is described in detail in Haase and others (2010b). The points were interpolated for a smooth soil thickness model in the uplands area, where eolian deposition of loess dominates, and interpolated for a smooth bedrock elevation model in the lowlands areas. These were combined with modifications made by hand to incorporate the steep contoured edges of the central bedrock valley based on individual high quality well logs. The perspective view shown in Figure 3 gives a good representation of the horizontal variability of the individual point measurements, and illustrates the difference in model surface complexity imposed for the uplands and lowlands. Cone penetrometer data with S-wave measurements (S-CPT) (Holzer, 2003) and borehole shear-wave velocity measurements (Eggert and others, 1994) were the primary source of data for determining the depth-dependent shear-wave velocities and are described in detail by Haase et al. (2010b). These data were separated into four groups based on the surficial geology. What we refer to as the river alluvium group (floodplain deposits) in the lowlands; the outwash terrace group includes terrace deposits at the edges of the Ohio River Valley; the lacustrine terrace group includes slackwater deposits of the lacustrine terraces; and the loess group includes eolian deposits over bedrock uplands. As shown by Haase et al. (2010b), the velocity variations are not large, with velocities in the 150 to 250 m/s range for the all groups, with uncertainties on the order of 60 m/s. Figure 4 shows the four reference velocity profiles used for the groups.

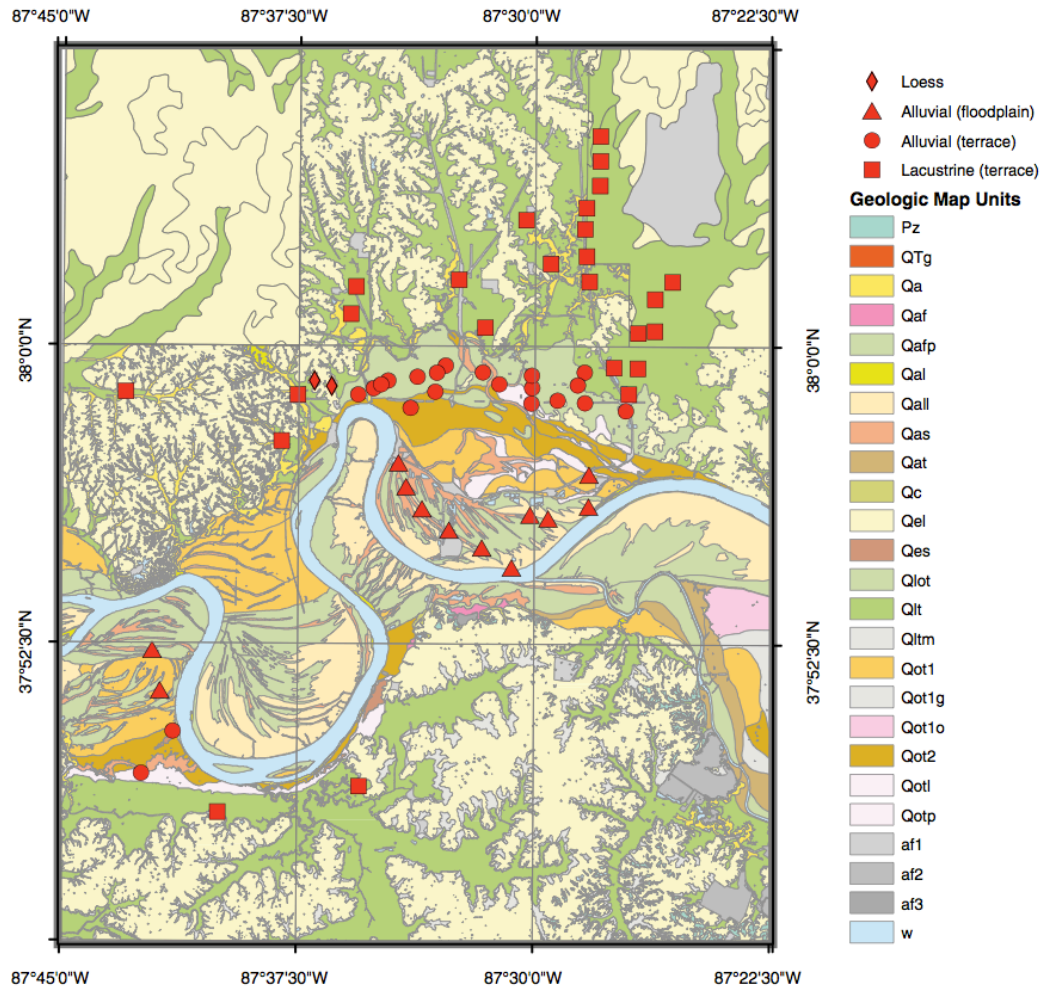


**Figure 1: Geological map of the study area. Red points indicate locations of S-CPT measurements of shear wave velocity.**

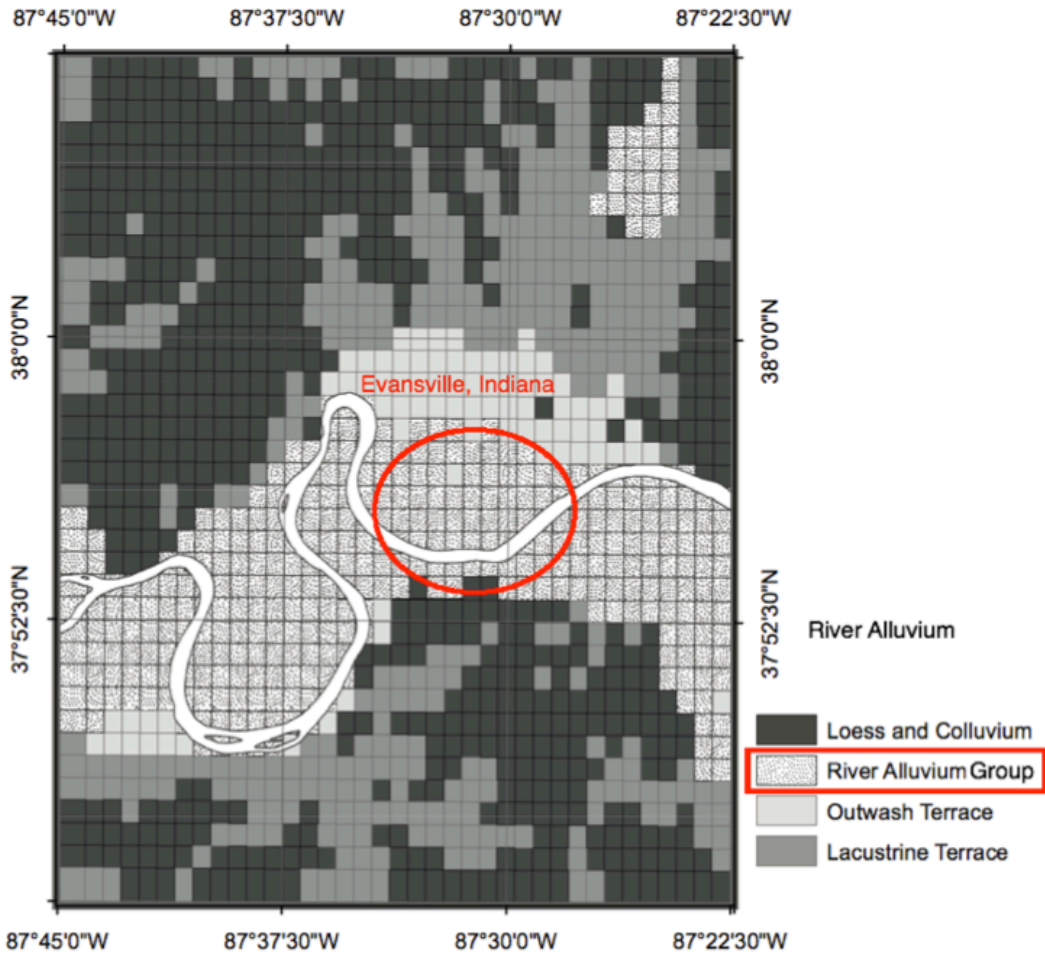


Figure 2: Assignment of velocity soils in the study area according to the surficial geology. The model discretized at 1km cell size was used in the 1D calculation of site response

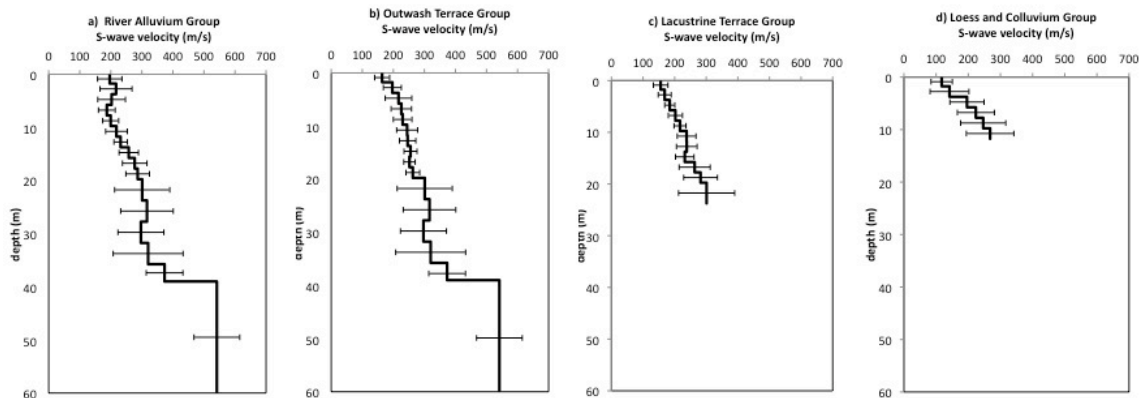


Figure 3 (Haase et al., 2011) shows the velocity profile above the bedrock for the River Alluvium Group, and the standard deviation of the measured shear-wave velocity. The four 1D velocity models used to construct the 3D model are described in Haase et al. 2011.

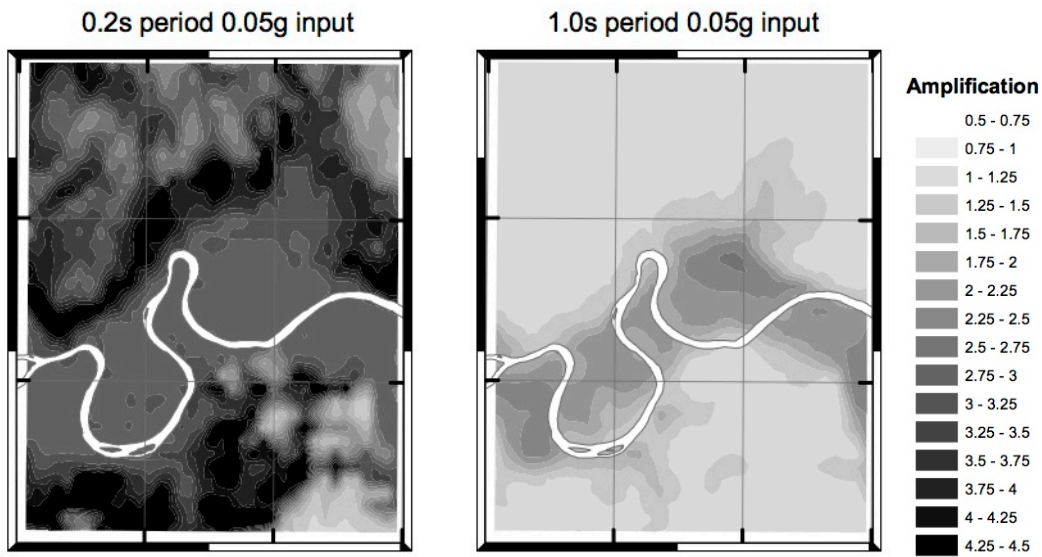


Figure 4: Amplification at 0.2s and 1.0s period (Haase et al, 2011).

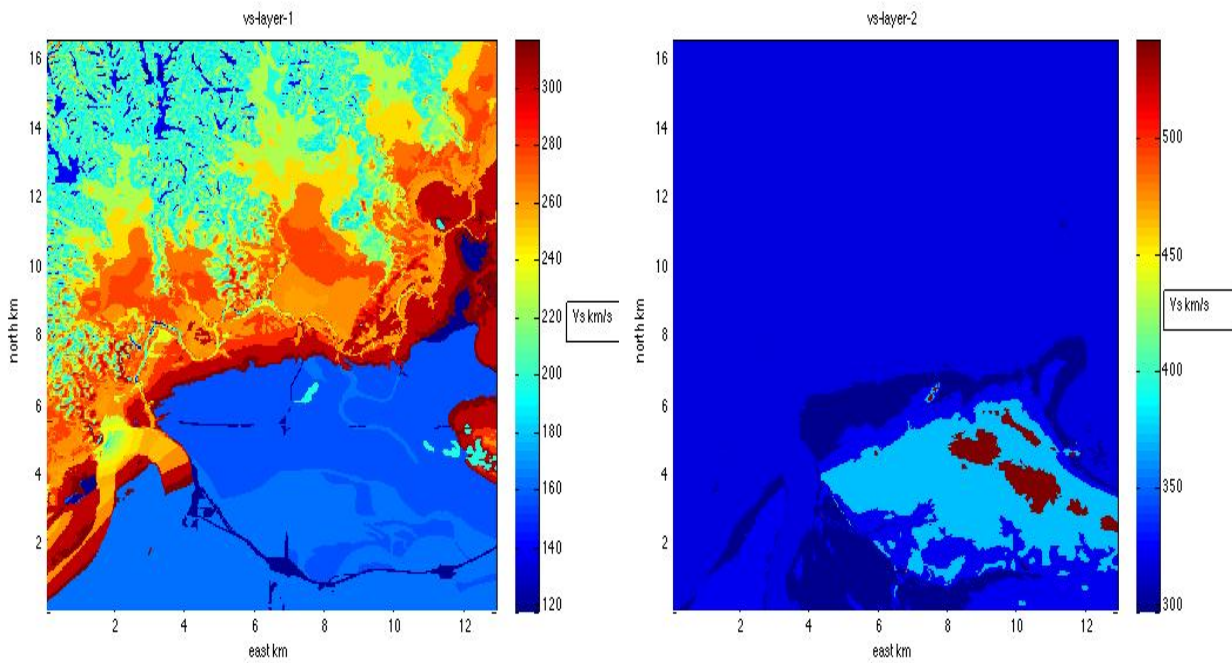


Figure 5 Shear wave velocity model for the northern boundary of the Ohio River flood plain used for the 3d wave propagation calculation, shown at 25m depth (left) and 50m depth (right).

The construction of the material media has been implemented with a fortran program that creates a 3D volume with the following parameters at each point: shear-wave velocity  $V_s$  and primary wave velocity  $V_p$ , the damping parameters  $Q_s$

for the shear-waves and Qp for the primary-waves, and the density rho. The program reads the 1 D velocity model appropriate for each point, ie. from Figure 5, and create a sequence of Vs and Vp according to the raster exported at the spatial discretization dh =25m. The value of Qp and Qs is assigned to 10000 so that there is almost no attenuation of energy (except at the boundaries). Vp values are determined based on a ratio of Vp/Vs, of 1.75. The contrast between the spatial discretization used for the previous calculation (Haase et al., 2011;) and the full 3D calculation (Figure 4) is clear.

### Method

The AWP-ODC code (Olsen et al., 1995) is able to simulate 3D wave propagation in a given medium. This scheme is fourth-order accurate in space and second-order accurate in time. With a staggered-grid finite difference scheme, the finite difference approach applied to wave propagation from Olsen solves the following 3D elasto-dynamic equations:

$$(1) \quad \partial_t v = \frac{1}{\rho} \nabla \cdot \sigma$$

$$(2) \quad \partial_t \sigma = \lambda(\nabla \cdot v)I + \mu(\nabla v + \nabla v^T)$$

where v is the ground motion, rho is the density, sigma is the stress tensor and lambda and mu are the Lamé's coefficients. Nine scalar-valued equations are coupled and theoretically we can determine the velocity vector and the stress tensor components. In practice, the code uses approximated finite difference equations:

$$(3) \quad \partial_t v(t) \approx \frac{v(t + \frac{\Delta t}{2}) - v(t - \frac{\Delta t}{2})}{\Delta t}$$

$$(4) \quad \partial_t \sigma(t + \frac{\Delta t}{2}) \approx \frac{\sigma(t + \Delta t) - \sigma(t)}{\Delta t}$$

It takes into account anelastic losses using frequency-dependent quality factors (Qs for the shear-waves and Qp for the primary-waves). As the study domain is truncated, Absorbing Boundary Conditions (ABC) are applied to the simulation to avoid multiple reflections. The AWP-ODC code provides two different types of ABCs: the Perfectly Matched Layer (PML) and Cerjan.

PMLs decomposes the two unknown variables into normal and tangential components so that we can get the following four equations (in this example, wave propagates in the x-direction):

$$(6) \quad \partial_t v^{\perp x} = \frac{1}{\rho} \nabla^{\perp x} \cdot \sigma$$

$$(7) \quad \partial_t v^{\parallel x} = \frac{1}{\rho} \nabla^{\parallel x} \cdot \sigma$$

$$(8) \quad \partial_t \sigma^{\perp x} = \lambda(\nabla^{\perp x} \cdot v)I + \mu(\nabla^{\perp x} \cdot v + \nabla^{\perp x} \cdot v^T)$$

Then a new term is added to equations (6) and (8) (the components that are perpendicular to the boundary):

$$(11) \quad \partial_t v^{\perp x} + d(x)v^{\perp x} = \frac{1}{\rho} \nabla^{\perp x} \cdot \sigma$$

$$(12) \quad \partial_t \sigma^{\perp x} + d(x)\sigma^{\perp x} = \lambda(\nabla^{\perp x} \cdot v)I + \mu(\nabla^{\perp x} \cdot v + \nabla^{\perp x} \cdot v^T)$$

where  $d(x)$  is the damping function.

The parameters used in this study are summarized in Table 1.

**Table 1: Simulation Parameters**

Simulation	Evansville 3D
min dh (m)	23.47
max dt (s)	0.005145
Vp_max (m/s)	2189
Vs_min (m/s)	117.3
length (m)	35000
l-grid points	1491
width (m)	45000
w-grid points	1917
depth (m)	2000
d-grid points	85
tot. grid points	259 522 560
source freq. (Hz)	0.5
min $\lambda$ (m)	234.7
N grid points per $\lambda$	10

Our specific work focuses on a study area that contains only the central quadrangle in Figure 1, nine times smaller than the full study area. The implementation for the Kraken and Lonestar SuperComputers require the total number of nodes in each direction to be a multiple of 12 in order to use the number of processors per node efficiently.

PMLs are more able to absorb waves near the boundaries than Cerjan, but can be unstable in the presence of strong gradients whereas Cerjan is always stable.

The first step of the work was to determine parameters such as grid spacing, and temporal discretization. The conditions for the Evansville project are  $V_{s_{\min}}$  and  $V_{p_{\max}}$ , and the model area length and width and depth. N is the number of grid points per wavelength. We chose a source frequency of 0.5 Hz and 10 grid points per wavelength ( $\lambda$ ). The minimum spatial discretization dh was determined by the choice of N and the period of the source:

$$\frac{\lambda_{\min}}{N} = dh \quad i.e$$

$$\frac{V_{s_{\min}} \cdot T_{source}}{N} = dh$$

The maximal temporal discretization  $dt$  was determined by the Courant-Friedrichs-Lewy condition:

$$V_{p_{\max}} \cdot \frac{dt}{dh} < 0.48 \quad and \quad dt_{\max} = \frac{0.48 \cdot dh}{V_{p_{\max}}}$$

Our specific work focused on a study area that contains only the central quadrangle in Figure 1, nine times smaller than the full study area. The implementation for the Kraken and Lonestar SuperComputers required the total number of nodes in each direction to be a multiple of 12 in order to use the number of processors per node efficiently.

**Table 2: Implementation of the Two Media**

medium	dh (m)	dt (s)	size (nodes)	velocity model
1D-varying	25	0.005	512*640*88	River Alluvium Group
Homogeneous	25	0.005	512*640*88	Vs=1251.1 m/s Vp/Vs=1.75
3D varying	25	0.005	516*661*88	Vs=1251.1 m/s Vp/Vs=1.75

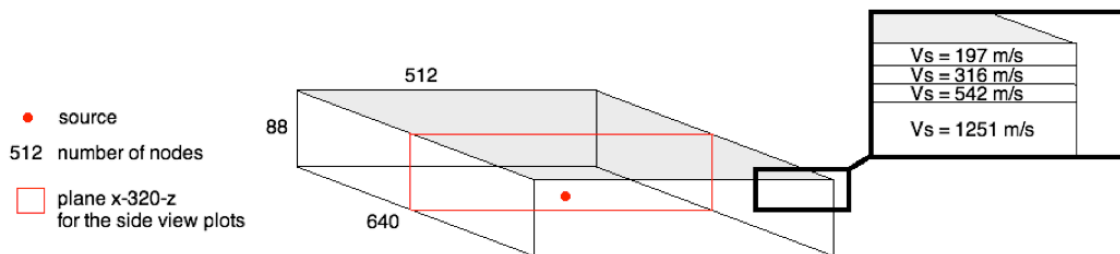


**Figure 6 3D Medium with 1D-varying Velocity**

The source was placed in the lower center of the rectangle. We allowed 28 nodes under the location of the source so that it was not located on layers that are dedicated to absorb energy (the last twenty layers at the bottom and on the sides). The source is a 1.0 s gaussian curve (Figure 5). Such a source creates a 2.0 s period perturbation in the medium.

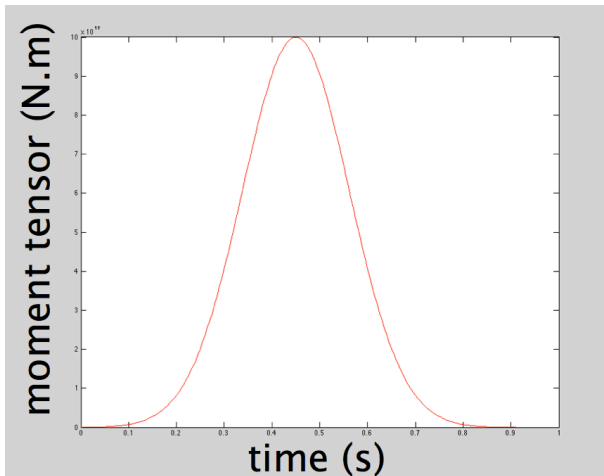


**Figure 7 Moment tensor time function used for the point source.**

To summarize, we tested the stability of the code in a medium where there is a large discontinuity in the shear-wave velocity. The test simulations (Table 2) were implemented with a 1D-varying velocity model because it is sufficient for testing numerical stability. The energy can propagate in every direction. The final simulations were implemented with a 3D-varying velocity model, according to the velocity soil distribution (Figure 4).

### *Results*

We plotted the ground motion velocity for a cross-sections, in the vertical output plane (Figure 4, in red) both cases scaled to 40 m/s, which is the maximum amplitude of the ground motion observed in the layered medium. Figure 6 shows the wave after it has propagated from the bottom to the surface through the homogeneous medium, at times 1.125 s, 1.525 s and 1.825 s. The energy propagating downwards is effectively absorbed in the absorbing layers and does not interfere with the interpretation of the ground motion near the surface. For the layered case, we obtain plots of ground motion that show evidence of trapped waves in the subsurface layers (Figure 7). The energy remains in the upper layers. Moreover, resonance and amplification of the seismic waves can be observed in these layers. Indeed, the amplitude remains at a high level (around 20 m/s) until time 1.825.

$$V_s = 1251.1 \text{ m/s} \quad V_p/V_s = 1.75$$

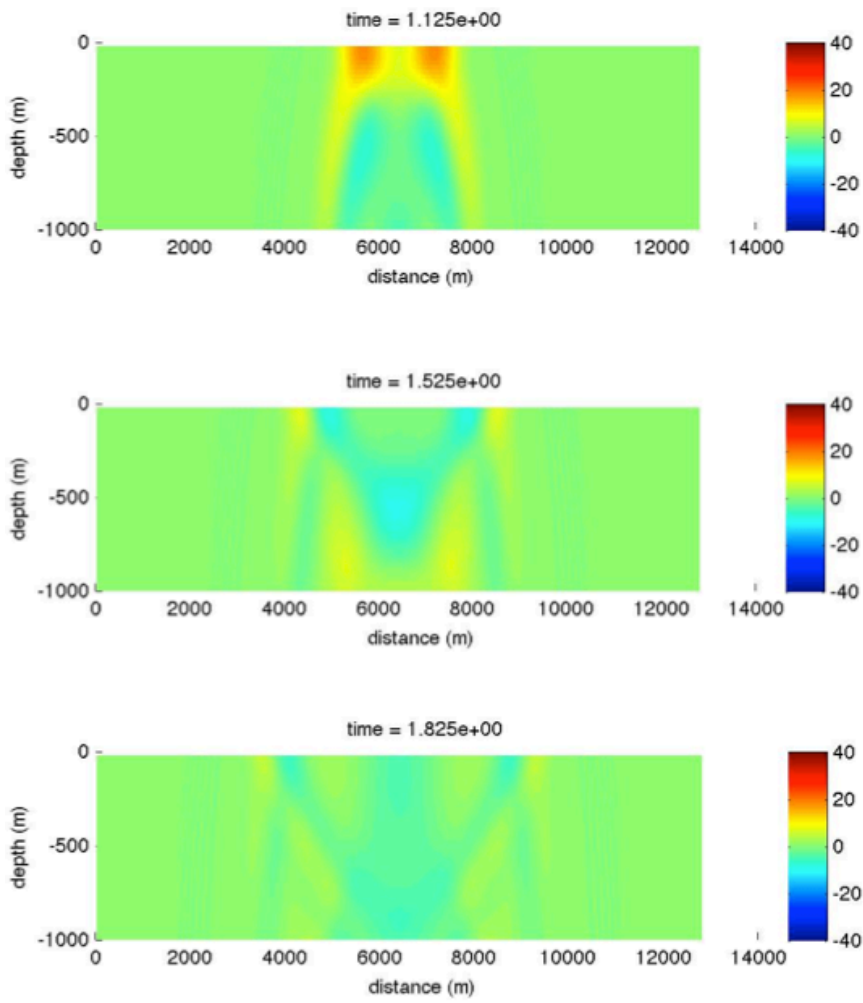
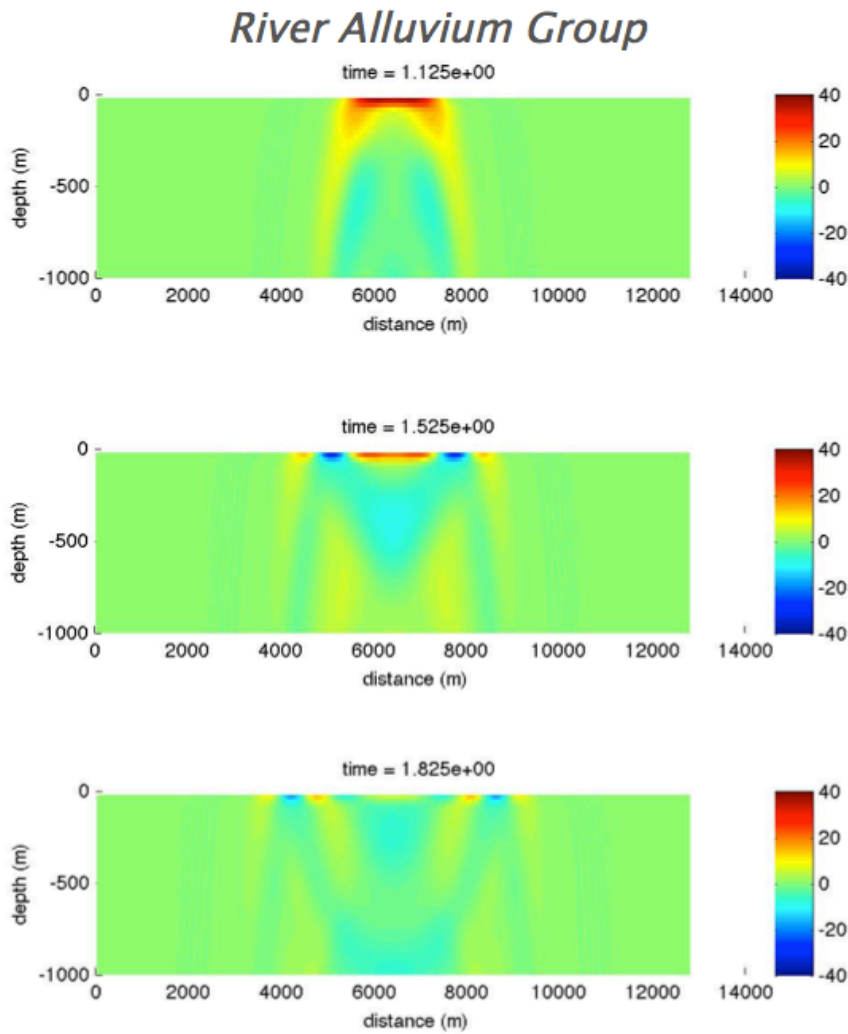
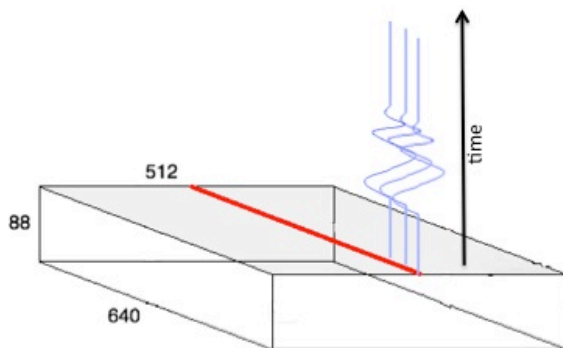


Figure 8 Cross-sections of the ground motion (m/s) for the homogeneous medium



**Figure 9** Cross-sections of the ground motion (m/s) for the 1D-varying medium

To better illustrate the longer duration of shaking in the 1D-varying case, we plotted record section along the North-South axis at the surface (Figure 8, in red).



**Figure 10** 3D Medium and Location of the Simulated Records.

Figure 9 displays the record sections for our two cases. The waveforms on the left clearly show multiple resonances following behind the initial wave front. To evaluate more precisely the duration of shaking, we plotted the time series for the two cases (Figure 10) at 750 m distance from the epicenter. We found that the time for the shaking to decrease to 10% of the maximum amplitude is 1.7 times longer for the layered model than in the homogeneous model.

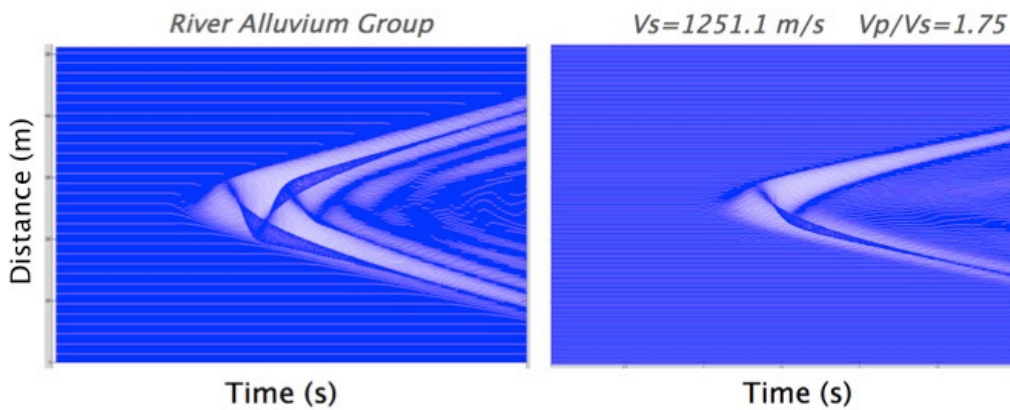


Figure 11 Record section for the 1D-varying (left) and the homogeneous (right) media

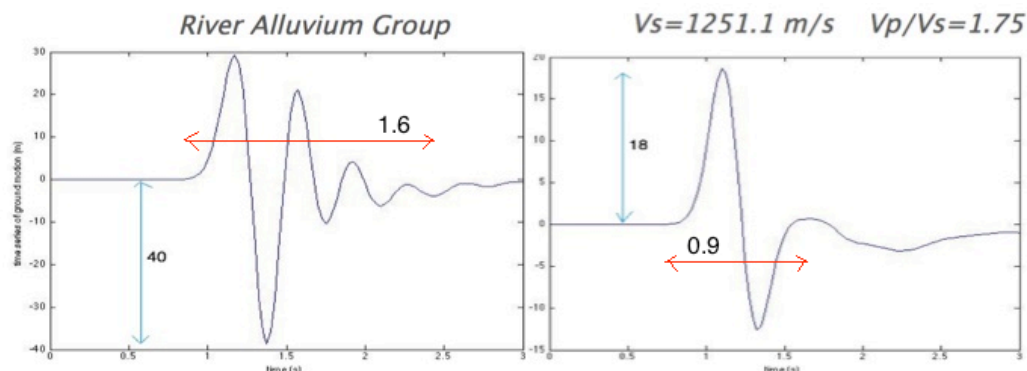


Figure 12 Time series of the ground motion for the homogeneous (left) and the 1D-varying (right) media

In the previous study (Figure 11, Haase and Nowack., 2011), the amplification factor was found to be within the same range in the center of the river alluvium for 1.0 s period {1.8; 4.6}. In our simulation, the maximum amplitude of the ground motion for the 1D-varying case was 40 m/s, and it was 18 m/s for the homogeneous case. So the amplification factor is 2.2, which makes our results consistent with what we expected.

We also predicted the central processing unit (CPU) time for general full 3D simulations by running several jobs and then scaling up the results. Table 3

summarizes the different parameters for different simulations. We obtained the predicted CPU time based on the formula:

$$\text{predicted CPU time (ii)} = \left( \frac{t_{\max,ii}}{t_{\max,i}} \cdot \frac{NX_{ii} \cdot NY_{ii} \cdot NZ_{ii}}{NX_i \cdot NY_i \cdot NZ_i} \cdot \frac{NP_i^3}{NP_{ii}^3} \right) \cdot \tau$$

where tau is the CPU time for case i (Table 3). NX is the number of nodes in the x direction. For cases ii to iv, the predictions are close to the actual CPU times. For cases v to vii, predicted CPU times are smaller by a factor of two, but the same order of magnitude. One of the reasons for this difference is that the performance of a computer is not linearly related to the number of processors NP for each direction. We expect the CPU time for the future simulation to be about half an hour, if we choose 9 s for tmax. Although the test case was for a source with minimum 2 s period, the previous calculation (Haase ...) was for shorter periods of engineering interest for smaller structures, specifically 1 s and shorter. The table shows that it may be feasible to push the calculations to these shorter periods.

	dh (m)	dt (s)	freq. (Hz)	tmax (s)	NX*NY*NZ	NP	Vs model	CPU time (s)	p. CPU time
i	200	0.01	0.5	4	128*128*128	2	a	28.26 = τ	
ii	200	0.01	0.5	4	256*256*256	2	a	222.139	226.1
iii	200	0.01	0.5	4	128*128*128	4	a	6.036	3.533
iv	200	0.005	0.5	8	128*128*128	2	a	61.128	56.52
v	200	0.005	0.5	8	256*256*256	2	a	733.975	452.2
vi	25	0.005	0.5	3	512*640*88	4	b	80.492	36.42
vii	25	0.005	0.5	3	512*640*88	4	c	76.413	36.42
viii	25	0.005	0.5	9	1536*1920*88	4	b	?	983.7
ix	12.5	0.005	1	9	3072*3840*176	4	b	?	7869.6
x	12.5	0.005	1	9	3072*3840*176	12	b	?	874.4

**Table 3: CPU time and Predicted CPU time for Several Simulations. a: Vs=3464m/s and Vp/Vs=1.73; b: River Alluvium Velocity Model; c: Vs=1251.1m/s and Vp/Vs=1.75**

### *Spectral analysis*

A spectral analysis was carried out to evaluate whether amplification was present in the observed seismic data. The event that was studied was a magnitude 3.9

earthquake in the New Madrid seismic zone on 21 February 2012. This was the largest event that had been recorded on multiple stations, since the NSF Earthscope transportable array was present in Indiana. Three sites had recordings: USIN, located in the uplands area with thin layers of loess, EVIN, located in the Ohio River terraces, primarily gravel and alluvium, and TCIN, located in the lacustrine deposits (Figure 13). The two sites (EVIN and TCIN) that are on deeper soils show amplification at about 2 Hz. Site TCIN, which is located on lacustrine soils, shows an additional amplification peak at around 5-6 Hz. These frequencies are consistent with resonance in soils with the range of thicknesses described by the 3D model. EVIN is located above alluvial soils nearby State routes 41 and 62, and is near enough to be representative of soils and site response typical of the conditions for that infrastructure. Three site observations are not sufficient to verify definitively that the 3D response calculated from the soil model, therefore further verification studies should be carried out. However, it indicates the results will be useful for understanding how amplification due to soils may affect major infrastructure in the region.

**Table 4 Earthquake locations for data used in the spectral analysis.**

DATE	O.T.	LAT	LONG	DEP	MAG
2/21/12	58:43.6	36.87333	-89.42267	7.81	3.9
2/21/12	18:18.1	36.86750	-89.41350	10.18	1.8
2/21/12	05:47.8	36.87150	-89.41683	10.14	2.5
2/21/12	38:04.0	36.87200	-89.40833	10.80	2

**Table 5 Stations in the study area with recordings available for the Feb 21 2013 event.**

STATION	OPERATION STARTTIME	LAT	LON	ELEVATION	
EVIN	1/1/11	0:00:00	37.9716	-87.5297	140.0
TCIN	10/21/10	0:00:00	38.0116	-87.5290	117.3
USIN	10/23/02	0:00:00	37.9650	-87.6660	170.7

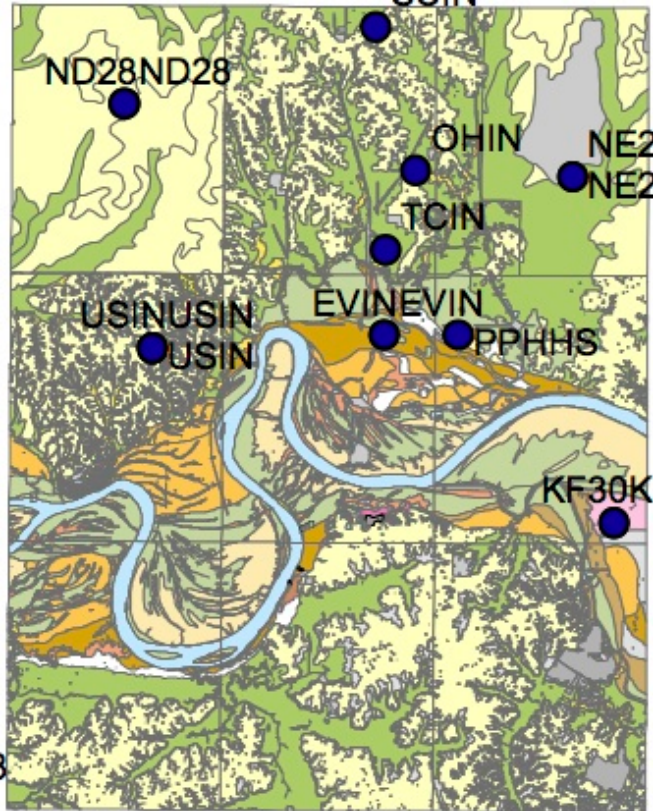


Figure 13 Seismic station locations. EVIN, TCIN, USIN were used in this study.

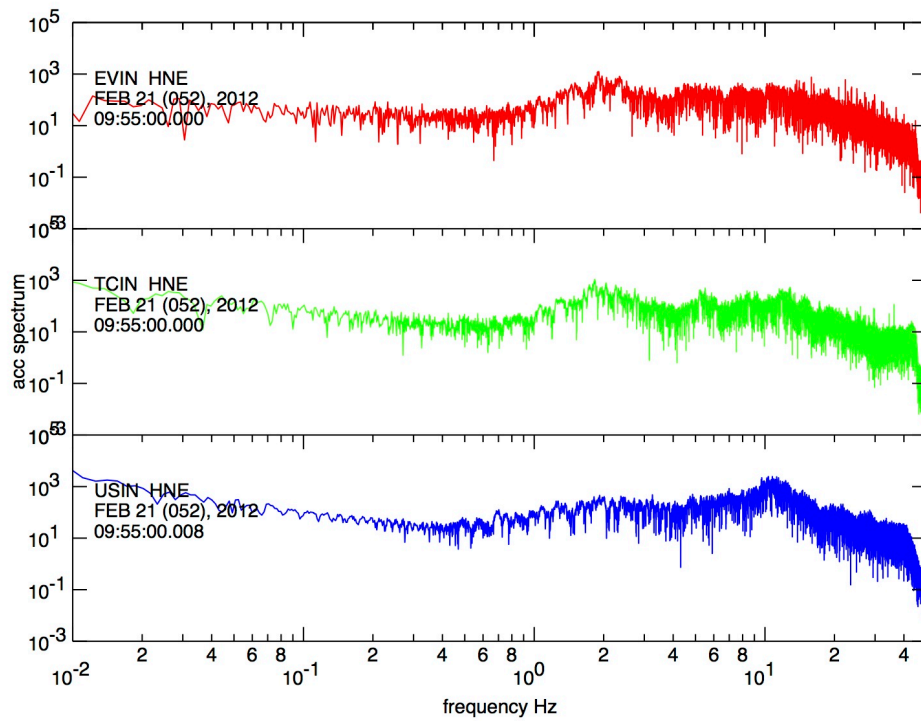


Figure 14 East component acceleration spectra from three sites in the Evansville area: EVIN, TCIN, USIN for the M3.9 New Madrid event on 21 February 2012.

### *Conclusion*

The objective of this study was to determine whether 3D simulations for the Evansville area produced amplified shaking with longer duration motions than 1D motions. We used the AWP-ODC finite difference code and submitted jobs to the Lonestar supercomputer (Univ. Texas) to calculate the ground motion data. We carried out runs for three types of media: a homogeneous model, a 1D-varying Vs model, and a full 3D calculation. We found that the amount of amplification is much greater, and so is the extended duration of shaking.

The result of this study was that it is actually possible to carry out a 3D simulation in the study area, provided we adjust parameters such as grid spacing to correct values. This simulation provides complementary information for updating the hazard maps of the Evansville area. The Evansville community, which is already committed to earthquake prevention, will have access to better tools to raise people's awareness about potential risks.

### *Acknowledgements*

Dr. Kim Olsen (San Diego State University) is thanked for his assistance for implementing the calculation. Support from postdoctoral researchers, including Supercomputer resources were provided under an XSEDE startup allocation and funding was provided by USGS NEHRP grant G12AP20150.

### *References*

- Bolt, Bruce A.. Earthquakes. New York: W. H. Freeman and Company, 1999. Print.
- Cui, Yifeng, et al. "Scalable earthquake simulation on petascale supercomputers." High Performance Computing, Networking, Storage and Analysis (SC), 2010 International Conference for. IEEE, 2010.
- Haase, Jennifer S., et al. "Probabilistic seismic-hazard assessment including site effects for Evansville, Indiana, and the surrounding region." Bulletin of the Seismological Society of America 101.3 (2011): 1039-1054.
- Haase, Jennifer S., and Robert L. Nowack. "Earthquake Scenario Ground Motions for the Urban Area of Evansville, Indiana." Seismological Research Letters 82.2 (2011): 177-187.

Haase, Jennifer S., Yoon Seok Choi, and Robert L. Nowack. "Liquefaction Hazard near the Ohio River from Midwestern Scenario Earthquakes." *Environmental & Engineering Geoscience* 17.2 (2011): 165-181.

Idriss, I. M., and J. I. Sun (1992), User's manual for SHAKE91Rep., 47 pp, Center for Geotechnical Modeling, Dept. of Civil and Environmental Engineering, University of California, Davis, CA.

Olsen, K. B., et al. "TeraShake2: Spontaneous rupture simulations of Mw 7.7 earthquakes on the southern San Andreas fault." *Bulletin of the Seismological Society of America* 98.3 (2008): 1162-1185.

Olsen, Kim B. "Final Report-NEHRP Award# G10AP00007."

Olsen, Kim B., James C. Pechmann, and Gerard T. Schuster. "Simulation of 3D elastic wave propagation in the Salt Lake Basin." *Bulletin of the Seismological Society of America* 85.6 (1995): 1688-1710.

Olson, Erik L., and Richard M. Allen. "The deterministic nature of earthquake rupture." *Nature* 438.7065 (2005): 212-215.

Stein, Seth and Wysession, Michael. *An Introduction to Seismology, Earthquakes, and Earth Structure*. Wiley, 2003. Print.